Electronic Supplementary Material (ESI) for Catalysis Science & Technology.

Supplementary Information

Kinetic and structural understanding of bulk and supported vanadium-based catalysts for furfural oxidation to maleic anhydride.

Oscar Gómez-Cápiro[a,b], Luis Bravo[a], Patricio Lagos[a], Paola Santander[a,b], Gina Pecchi[b,c], Alejandro Karelovic[a,b,d*]

[a]Carbon and Catalysis Laboratory (CarboCat), Department of Chemical Engineering, University of Concepción, Concepción, Chile

[b]Millennium Nuclei on Catalytic Process towards Sustainable Chemistry (CSC), Chile.

[c]Physical Chemistry Department, Faculty of Chemical Sciences, University of Concepción, Chile

[d]Unidad de Desarrollo Tecnológico (UDT), Universidad de Concepción, Chile

---

*Corresponding author at: Carbon and Catalysis Laboratory (CarboCat), Department of Chemical Engineering, University of Concepción, Concepción, Chile. E-mail address: akarelov@udec.cl (A. Karelovic).

Supplementary Information

S1. Mass transfer limitations.

S1.1. Internal diffusion limitations.

The Weisz-Prater criterion (N_{WP}) (*Eq. S1*) was calculated to evaluate the extent of internal diffusion limitations during the reaction [1].

$$N_{WP} = \frac{r_{obs} \times R_P^2}{C_S D_{eff}} < 0.3 \qquad \text{(S1)}$$

Where:

r_{obs} : observed reaction rate (mol cm^{-3} s^{-1})

R_P : particle radii (cm)

C_s : surface concentration (mol cm^{-3})

D_{eff} : effective diffusion (cm^2 s^{-1})

The reaction rate chosen is the higher measured, in this case, corresponds to the V_2O_5/Al_2O_3 catalyst at 320°C. At these conditions:

$$r_{obs} = 5.42 \times 10^{-8} \frac{mol}{cm^3 s}$$

The particle diameter (d_P) range is between 150 and 380 µm, and the calculation was made with the higher value:

$$R_P = 0.019\ cm$$

The surface concentration was close to that of CO_2 in the catalytic bed:

$$C_S = 1.63061 \times 10^{-8} \frac{mol}{cm^3}$$

The effective diffusion (D_{eff}) (*Eq. S2*) for pores of the size measured in this work (**Table S3**) is governed by Knudsen diffusion (D_{Kn}) as follow:

$$D_{eff} = D_{Kn} = \frac{\bar{v} \times d_P}{3} \qquad \text{(S2)}$$

where $\bar{v}$ is the average gas rate, defined according to the *Eq. S3*:

$$\bar{v} = \left(\frac{8 \times k_B \times T}{\pi \times m}\right)^{1/2} \qquad \text{(S3)}$$

Knowing that k_B is the Boltzmann constant and m is the mass of molecular species, the average gas rate is:

$$\bar{v} = 31323.64 \frac{cm}{s}$$

Therefore, the Weisz-Prater criterion is:

$$N_{WP} = 0.0471 < 0.3$$

This allowed the discarding of the internal diffusion limitation.

S1.2. External diffusion limitations.

The influence of external diffusion limitation was corroborated by Mears criterion (*M*) (*Eq. S4*).

$$M = \frac{r_{obs} \times R_P \times n}{k_m C_r} < 0.15 \qquad \text{(S4)}$$

Where:

C_r : is the limiting reagent concentration in the fluid (mol cm^{-3})

n : is the reaction order

k_m : is the mass transfer coefficient (m s^{-1})

The mass transfer coefficient can be obtained from the dimensionless number of Sherwood (*Sh*), which is also a function of the Reynolds (*Re*) and the Schmidt (*Sc*) numbers (*Eq. S6 -S8*) and is defined according to:

$$Sh = \frac{k_m \times d_P}{D_f} \qquad \text{(S5)}$$

$$Sh = 2 + 0.6Re^{1/2} \times Sc^{1/3} \qquad \text{(S6)}$$

$$Re = \frac{\rho_f \times u \times d_P}{\mu_f} \qquad \text{(S7)}$$

$$Sc = \frac{\mu_f}{D_f \times \rho_f} \qquad \text{(S8)}$$

The density (ρ_f) and the viscosity (μ_f) of the gaseous mixture fed were calculated considering ideal gas behavior:

$$\rho_f = 1.96 \frac{kg}{m^3}$$

$$\mu_f = 1.88 \times 10^{-5}\, Pa \times s$$

The flow rate (*u*) is estimated from the volumetric flow (F_t) fed and the transverse area (A_t) of the reactor:

$$u = \frac{F_t}{A_t} = \frac{7.29 \times 10^{-7}}{7.09 \times 10^{-5}} = 0.0103\frac{m}{s}$$

Replacing the values in the *Eq. S7* and *Eq. S8* is possible to find the *Re* and the *Sc* numbers to calculate the *Sh* number using the *Eq. S6*.

$$Sh = 2 + 0.6 \times (5.37 \times 10^{-3})^{1/2} \times 1.1^{1/3} = 2.05$$

Then, it is possible to obtain the k_m value through the *Eq. S5*.

$$k_m = 3.56\frac{m}{s}$$

Finally, the Mears criterion is:

$$M = 0.0103 < 0.15$$

This allowed the discarding of the external diffusion limitation, as well.

S2.Carbon balance.

The carbon balance was developed as show equation *S9* (*Eq. S9*).

$$\%C = \frac{5\,\dot{n}^{0}_{fur}}{5\,\dot{n}_{fur} + 4\,\dot{n}_{MA} + \dot{n}_{CO_2} + \dot{n}_{CO}}\,100$$

Where $\dot{n}^0_{fur}$ is the molar flow of furfural at the inlet of the reactor, $\dot{n}_{fur}$ is the molar flow of furfural in the exhaust, $\dot{n}_{MA}$ is the molar flow of MA in the exhaust, $\dot{n}_{CO2}$ is the molar flow of carbon dioxide in the exhaust and $\dot{n}_{CO}$ is the carbon monoxide in the exhaust.

S3. The objective function and optimization parameters.

The objective function (*O.F.*), used to calculate the error for each model tested, is presented in equation (*Eq. S10*).

$$O.F. = \frac{\left(\sum\frac{\left|P_{fur\,exp} - P_{fur\,calc}\right|}{P_{fur\,exp}}\right) + \left(\sum\frac{\left|P_{MA\,exp} - P_{MA\,calc}\right|}{P_{MA\,exp}}\right)}{18} \times 100 \qquad \text{(S10)}$$

O.F. is included in a MATLAB® function, which in turn calls another MATLAB® function containing the first-order reaction model. The optimization can be accomplished in different ways; in this case, a genetic algorithm was used with the configuration shown in **Table S1**.

Table S1. Options for the genetic algorithm using the MATLAB® software (*ga* command of the Optimization Toolbox).

Options	Value		
EliteCount	0.05*PopulationSize		
FitnessLimit	-Inf		
FitnessScalingFcn	@fitscalingrank	[]	
HybridFcn	@fmincon	[]	
MaxStallTime	Inf		
NonlinearConstraintAlgorithm	'auglag'		
PlotFcn	[]		
SelectionFcn	@selectionstochunif		
ConstraintTolerance	1.0e-03		
CreationFcn	@gacreationuniform		
CrossoverFcn	@crossoverscattered		
CrossoverFraction	0.8		
Display	Off		
FunctionTolerance	1.0e-06		
InitialPopulationMatrix	1 × number of parameters to optimize		
InitialPopulationRange	[]		
InitialScoresMatrix	[]		
MaxGenerations	200 × number of parameters to optimize		
MaxStallGenerations	50		
MaxTime	Inf		
MutationFcn	@mutationgaussian	1	1
OutputFcn	[]		
PopulationSize	400		
PopulationType	'doubleVector'		
UseParallel	0		
UseVectorized	0		

The optimization bounds were defined as shown in **Table S2**.

Table S2. Optimization bounds for each parameter.

Optimization parameters	Lower limit	Upper limit
k_i	0.0000001	0.1
Ea_i(kJ mol^{-1})*	10	250

*The correspondent value of Ea_i were multiplied by 1000 into the model to obtain values in an order of magnitude closer to the kinetics constants.

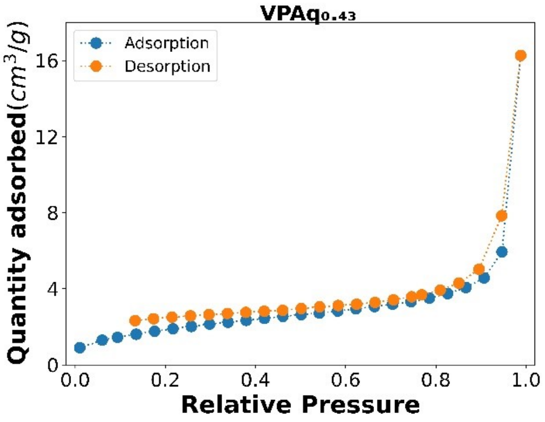
VPAq$_{0.43}$
Adsorption
Desorption
Quantity adsorbed(cm^3/g)
0
4
8
12
16
0.0
0.2
0.4
0.6
0.8
1.0
Relative Pressure

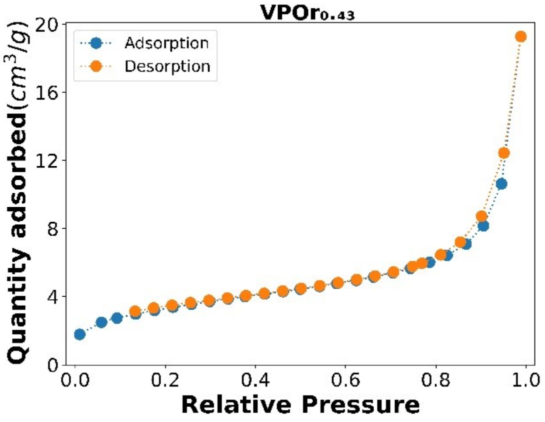
VPOr$_{0.43}$
Adsorption
Desorption
Quantity adsorbed(cm^3/g)
0
4
8
12
16
20
0.0
0.2
0.4
0.6
0.8
1.0
Relative Pressure

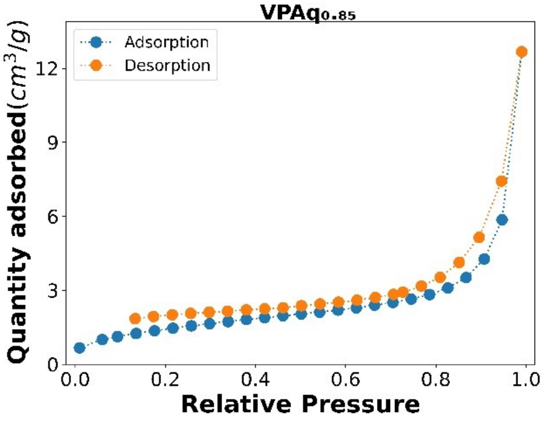
VPAq$_{0.85}$
Adsorption
Desorption
Quantity adsorbed(cm^3/g)
0
3
6
9
12
0.0
0.2
0.4
0.6
0.8
1.0
Relative Pressure

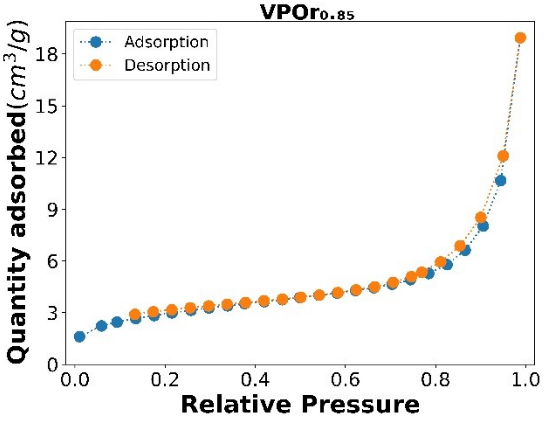
VPOr$_{0.85}$
Adsorption
Desorption
Quantity adsorbed(cm^3/g)
0
3
6
9
12
15
18
0.0
0.2
0.4
0.6
0.8
1.0
Relative Pressure

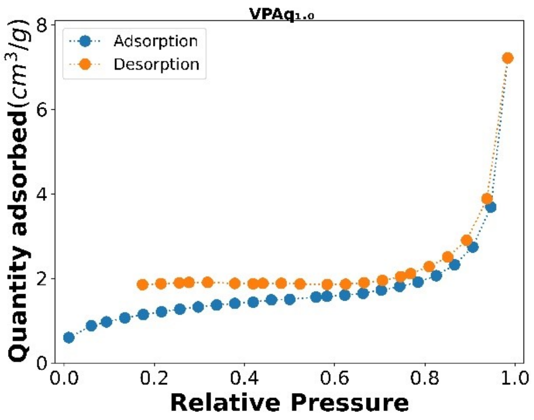
VPAq$_{1.0}$
Adsorption
Desorption
Quantity adsorbed(cm^3/g)
0
2
4
6
8
0.0
0.2
0.4
0.6
0.8
1.0
Relative Pressure

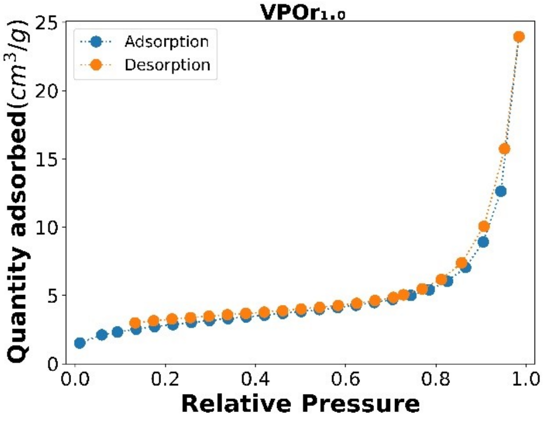
VPOr$_{1.0}$
Adsorption
Desorption
Quantity adsorbed(cm^3/g)
0
5
10
15
20
25
0.0
0.2
0.4
0.6
0.8
1.0
Relative Pressure

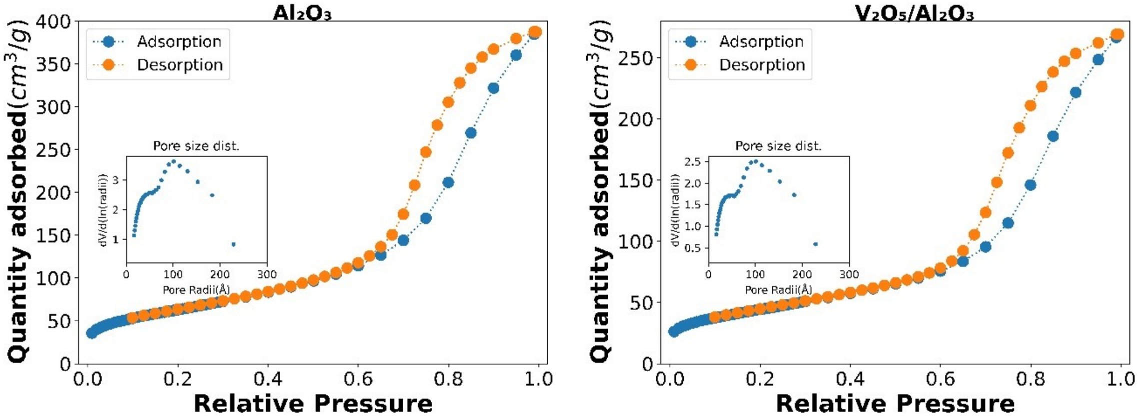

Figure S1. N_2 adsorption-desorption isotherms at 77K and pore size distribution for VPAq (P/V=0.43, 0.85, 1.00), VPOr (P/V=0.43, 0.85, 1.00), and V_2O_5/Al_2O_3 catalysts. Desorption branch of VPAq and VPOr isotherms were excluded since do not differ from the adsorption branch.

Table S3. Morphological properties of VPAq and VPOr catalysts

Catalysts	Specific surface area by BET (m²/g)	Pore Volume (cm³/g)	Pore Radii (nm)*
$VPAq_{0.43}$	6±0.12	0.27	90
$VPAq_{0.85}$	5±0.1	0.26	104
$VPAq_{1.00}$	4±0.08	0.16	80
$VPOr_{0.43}$	11±0.22	0.47	85
$VPOr_{0.85}$	10±0.2	0.48	96
$VPOr_{1.00}$	10±0.2	0.56	112
V_2O_5/Al_2O_3	158±0.95	0.407	7.6

* For V-P-O catalysts: hydraulic pore radii determined by Gurvitsch rule. For V_2O_5/Al_2O_3 catalysts: average pore size determined by the BJH method.

$VPA_{0.43}$

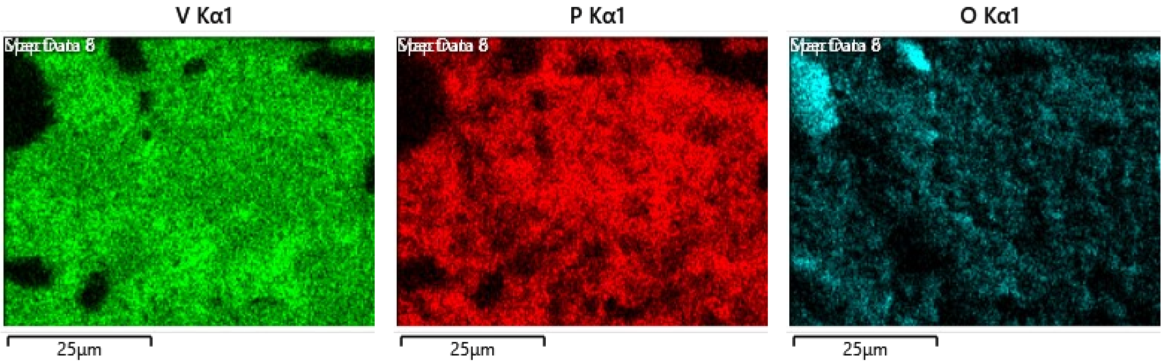

$VPA_{0.85}$

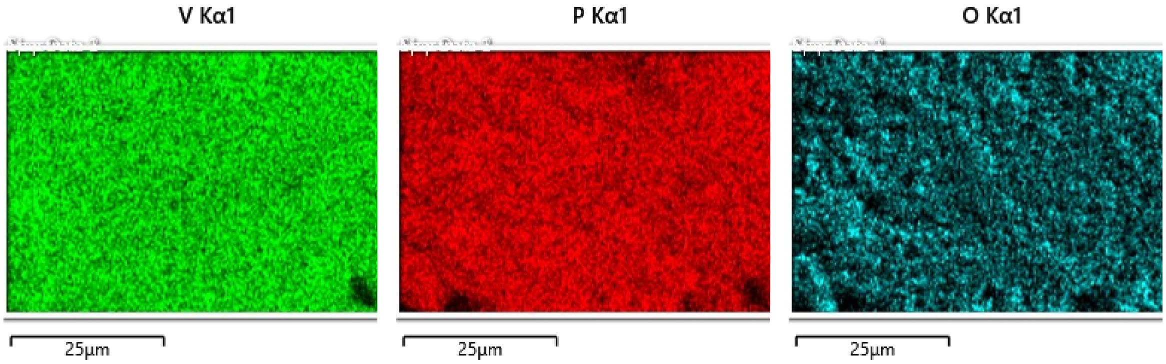

VPA$_{1.0}$

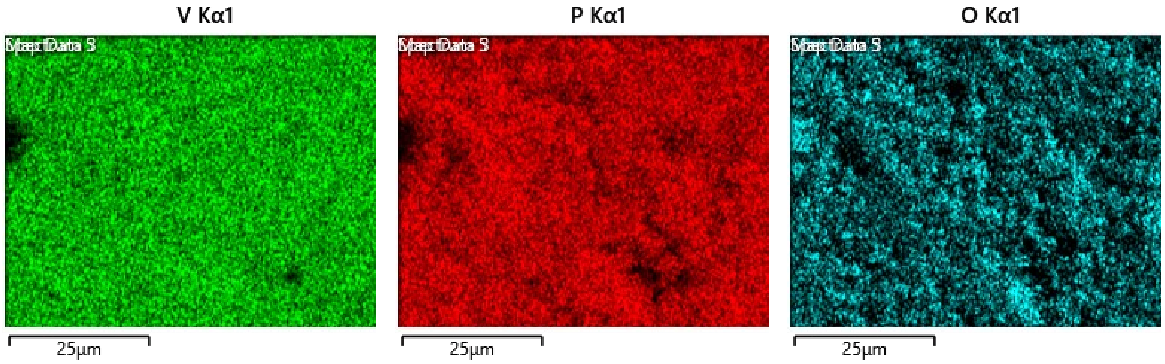

Figure S2. Screenshot of SEM-EDS mapping of bulk catalysts.

VPO$_{0.43}$

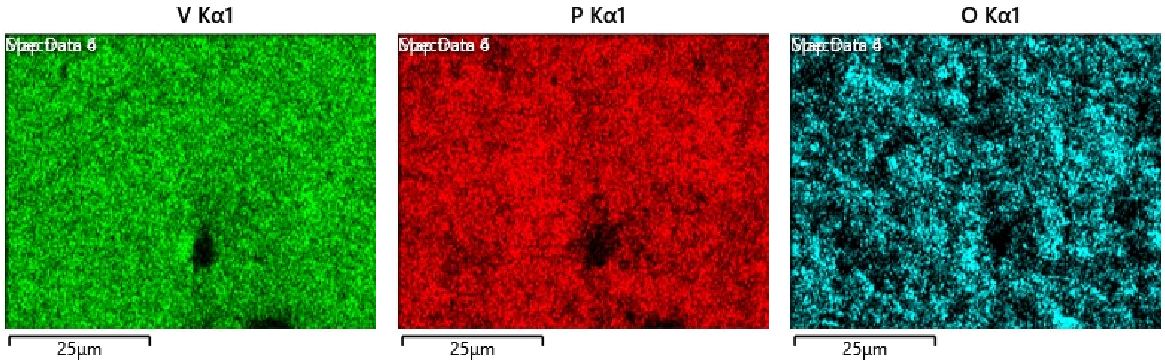

VPO$_{0.85}$

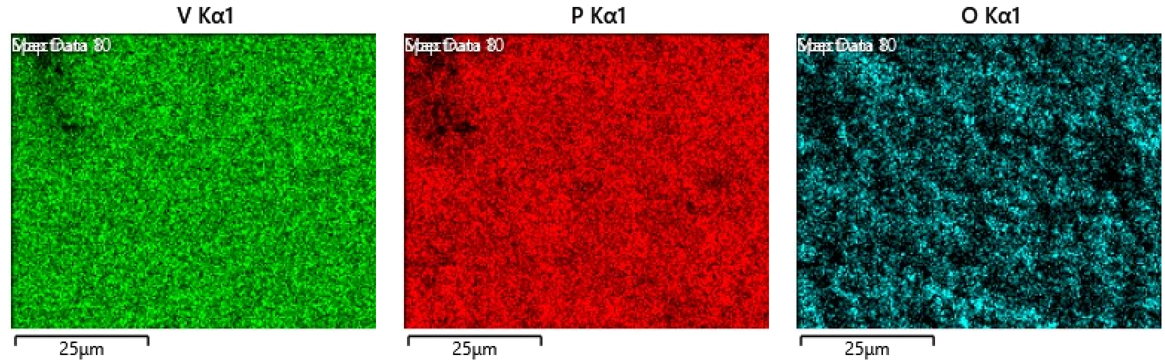

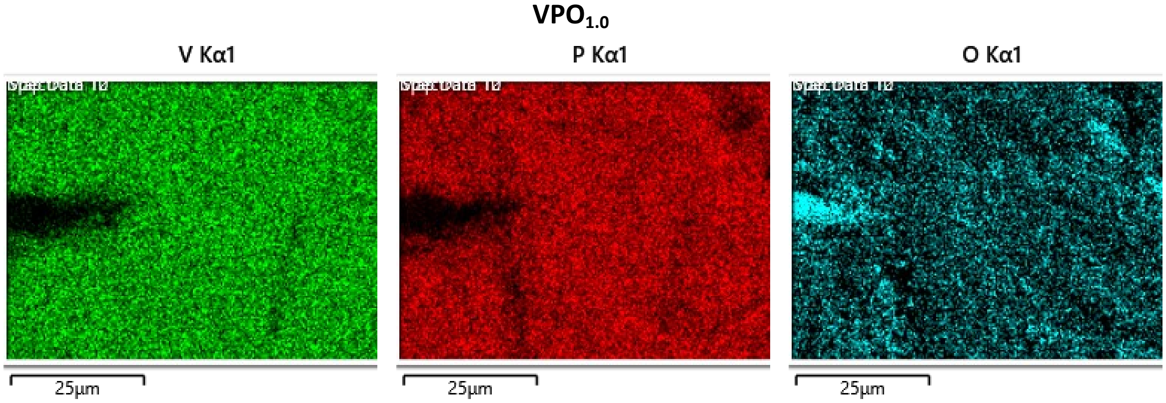

Figure S2. Screenshot of SEM-EDS mapping of bulk catalysts. (Continuation)

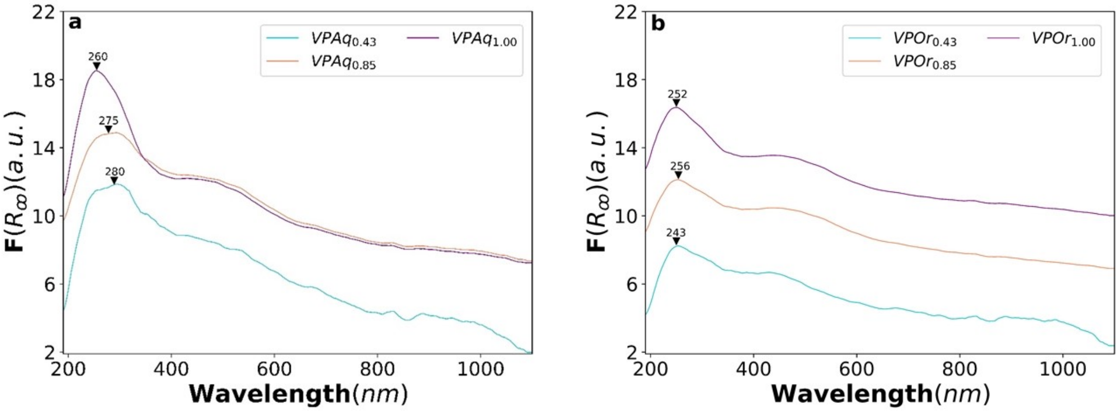

Figure S3. UV-vis DRS showing the maximum absorption wavelength values for (a) VPAq and (b) VPOr catalysts.

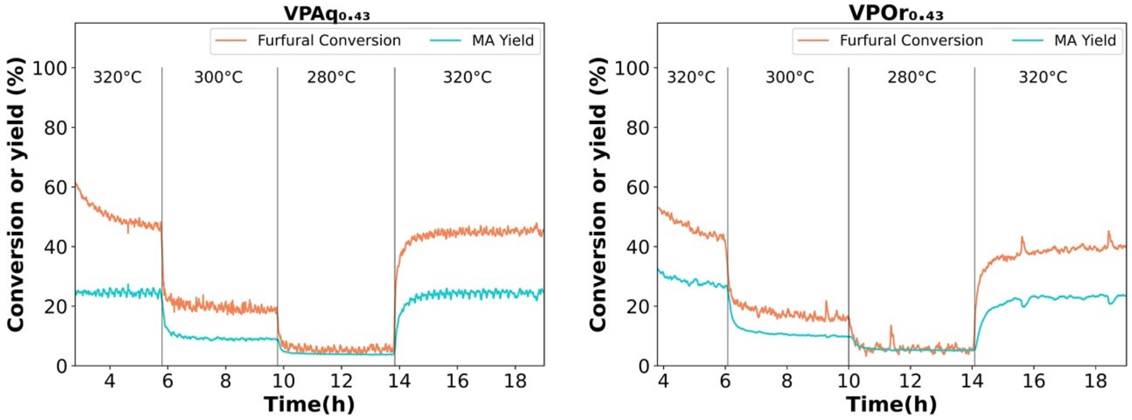

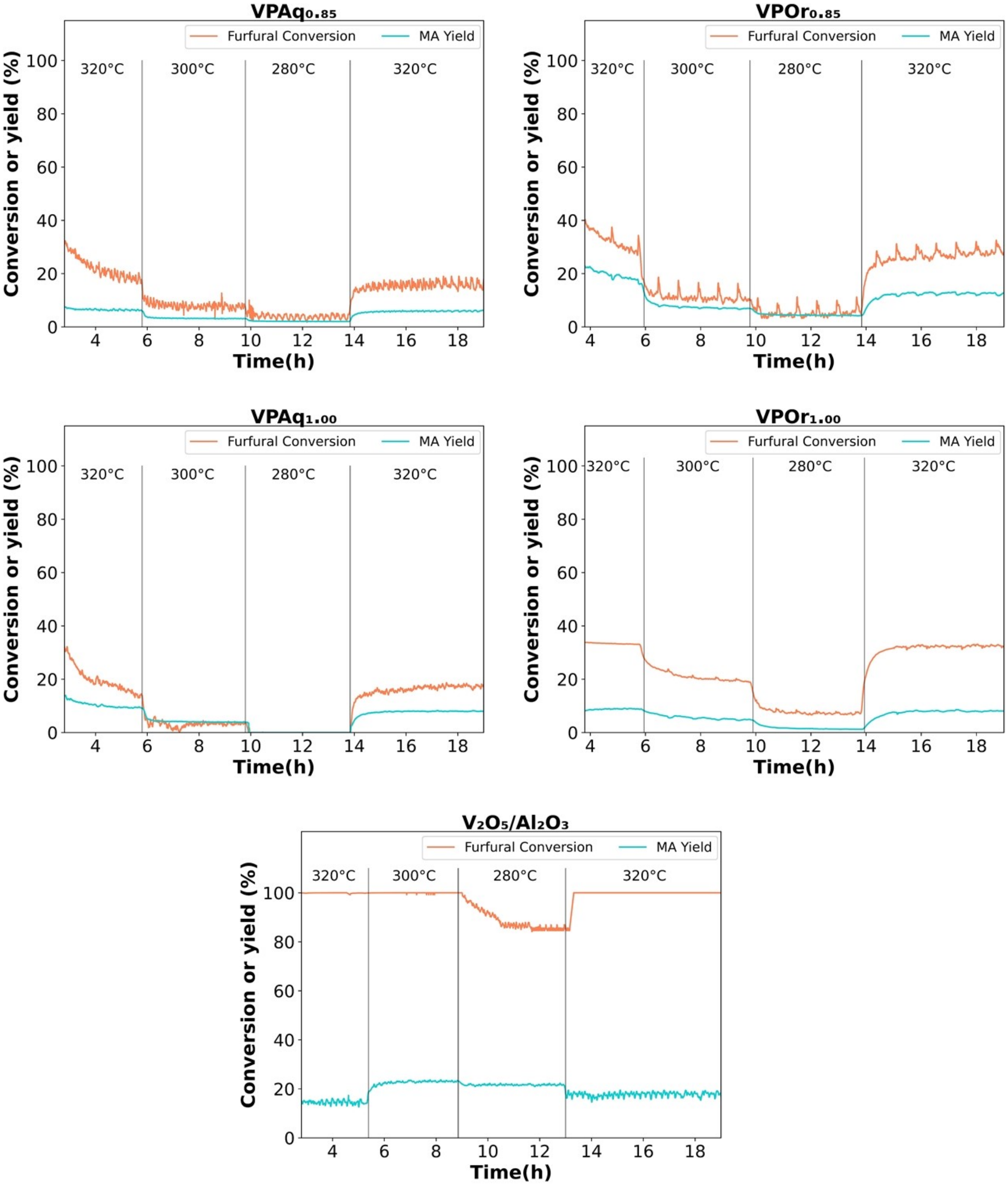

Figure S4. Furfural conversion and MA yield for VPAr, VPOr and V_2O_5/Al_2O_3 catalysts. P_{O2}/P_{fur} ratio=20, W/F=1.81 min mg_{cat} mL^{-1}.

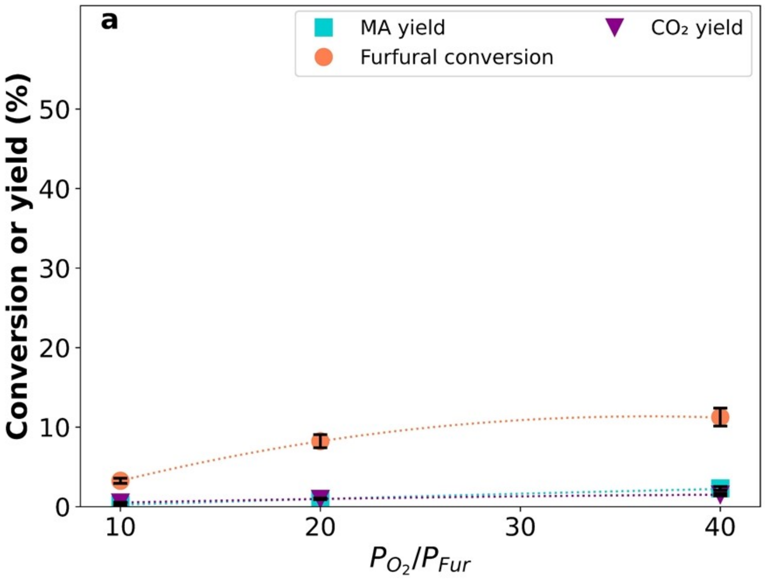
a
MA yield
Furfural conversion
CO₂ yield
Conversion or yield (%)
0
10
20
30
40
50
10
20
30
40
P_{O_2}/P_{Fur}

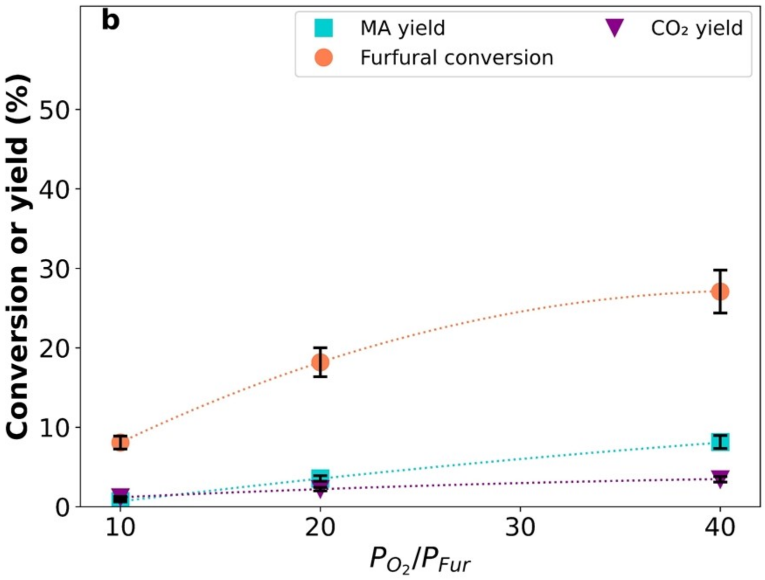
b
MA yield
Furfural conversion
CO₂ yield
Conversion or yield (%)
0
10
20
30
40
50
10
20
30
40
P_{O_2}/P_{Fur}

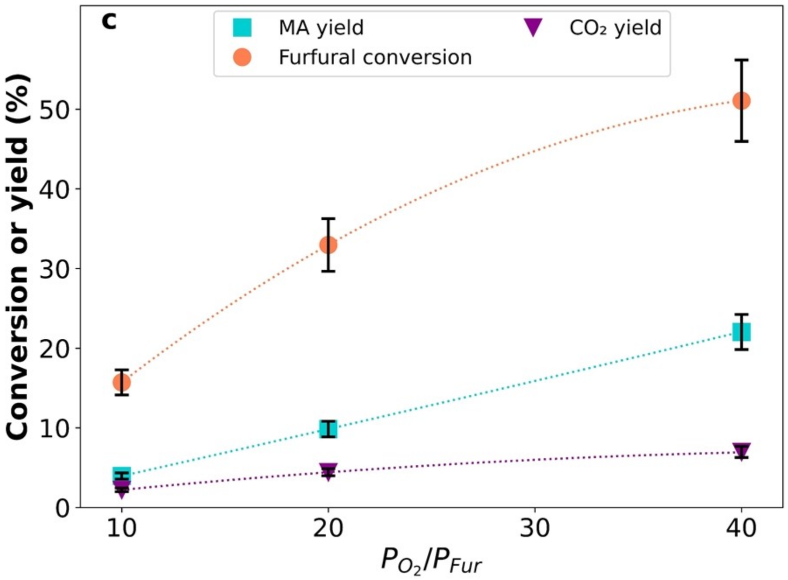

Figure S5. Effect of the P_{O2}/P_{fur} ratio (10, 20 and 40) at different reaction temperatures (a) 280°C, (b) 300°C and (c) 320°C on furfural conversion, MA yield, and CO_2 yield over $VPOr_{1.0}$ catalyst (W/F=1.81 min mg_{cat} mL^{-1}). The lines are added to show the trend.

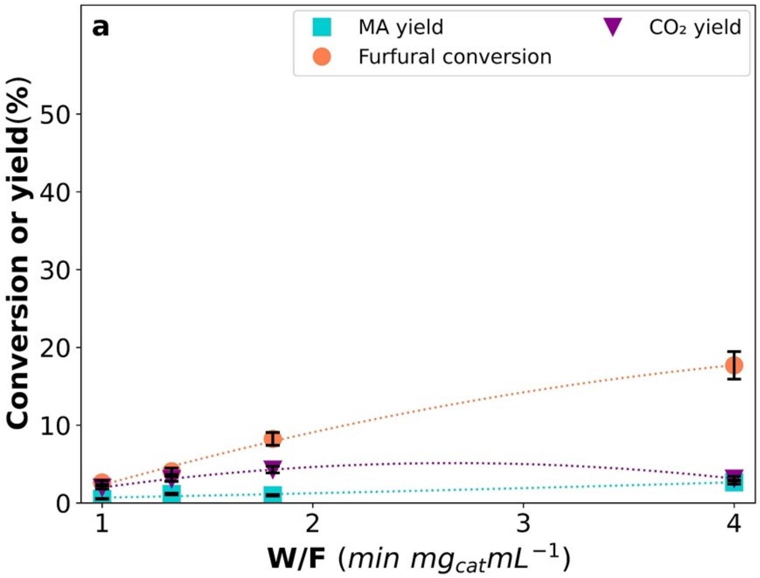

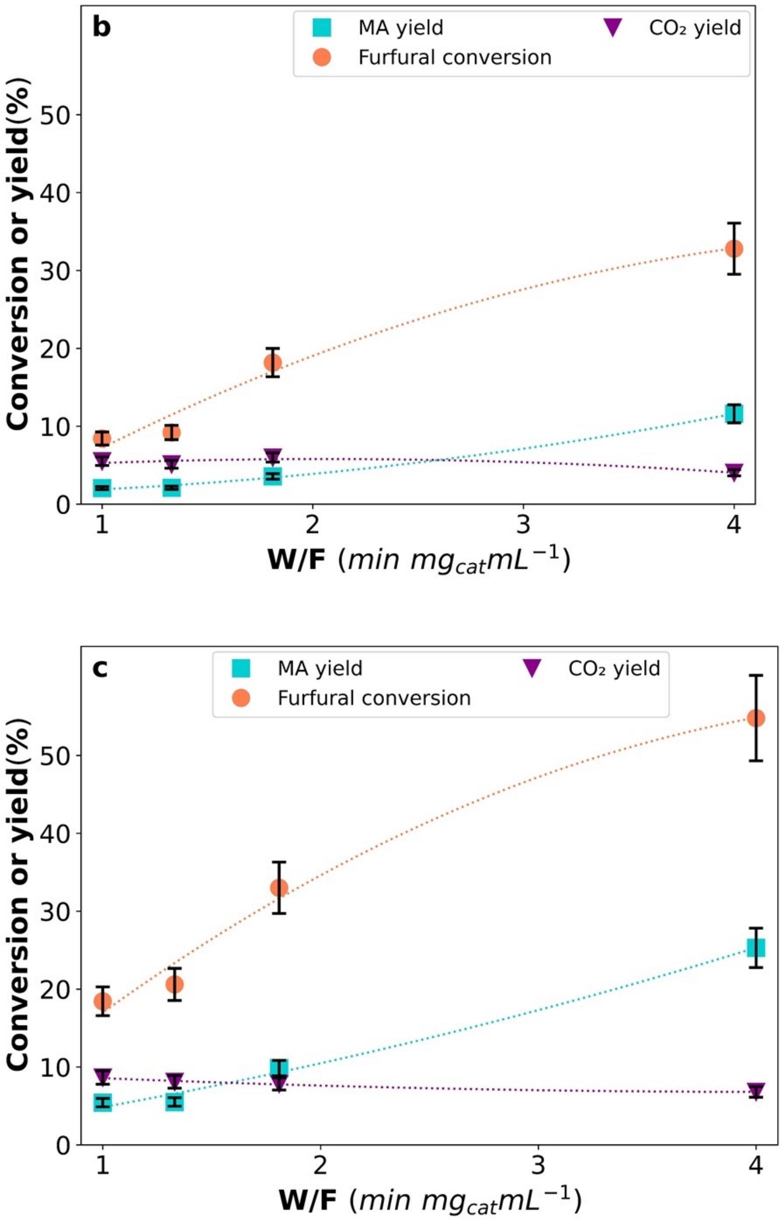

Figure S6. Effect of the W/F ratio (1, 1.33, 1.81 and 4 min mg_{cat} mL^{-1}) at different reaction temperature (a) 280°C, (b) 300°C and (c) 320°C on furfural conversion, MA yield and CO_2 yield over $VPOr_{1.0}$ catalyst (P_{O2}/P_{fur}=20). The lines are added to show the trend.

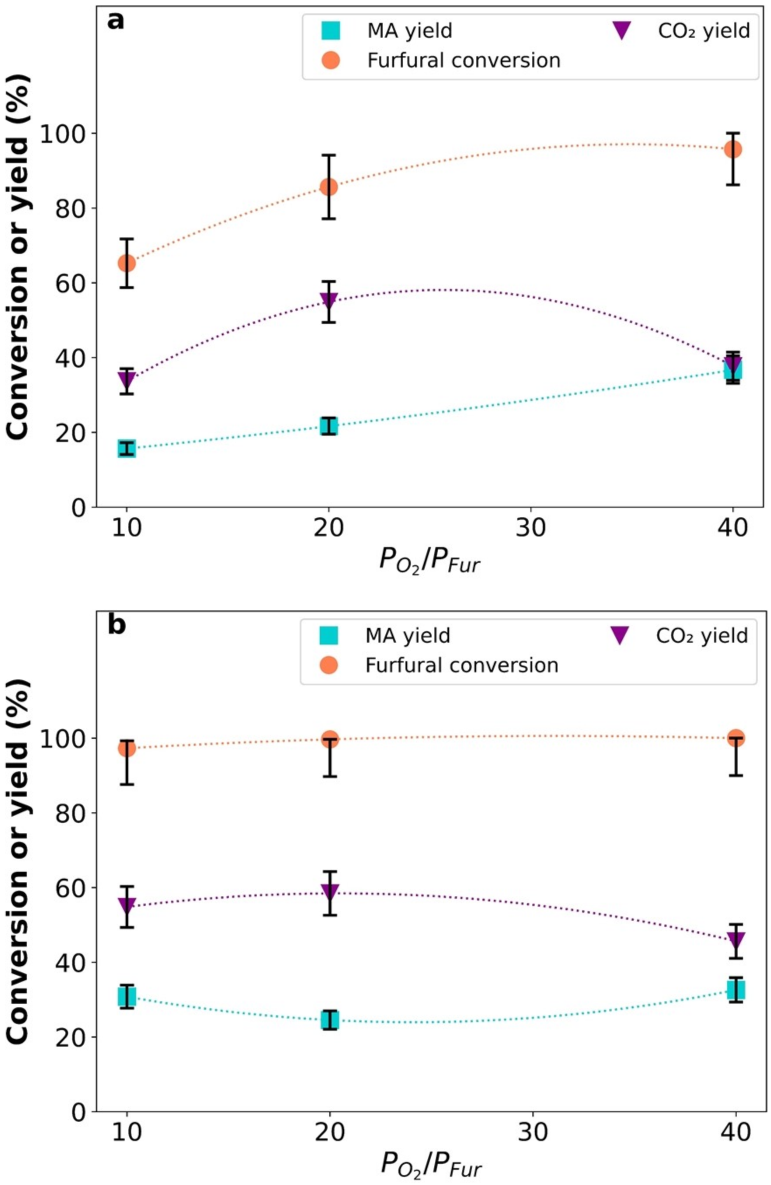
a
MA yield
Furfural conversion
CO₂ yield
Conversion or yield (%)
0
20
40
60
80
100
10
20
30
40
P_{O_2}/P_{Fur}
b
MA yield
Furfural conversion
CO₂ yield
Conversion or yield (%)
0
20
40
60
80
100
10
20
30
40
P_{O_2}/P_{Fur}

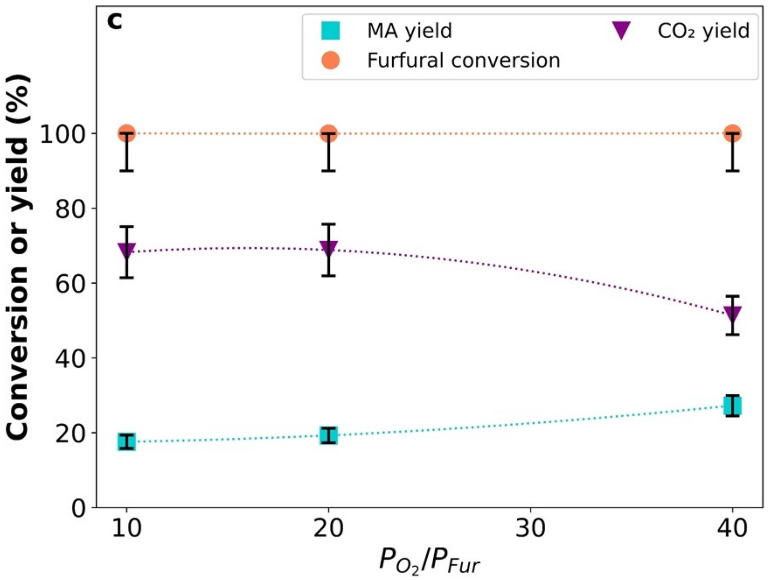

Figure S7. Effect of the P_{O2}/P_{fur} ratio (10, 20 and 40) at different temperatures (a) 280°C, (b) 300°C and (c) 320°C on furfural conversion, MA yield, and CO_2 yield over V_2O_5/Al_2O_3 catalyst (W/F=1.81, min mg_{cat} mL^{-1}). The lines are added to show the trend.

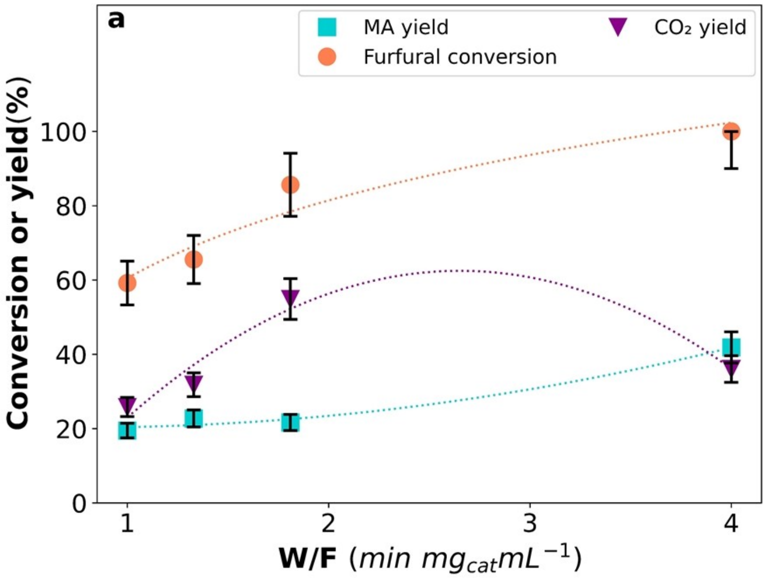

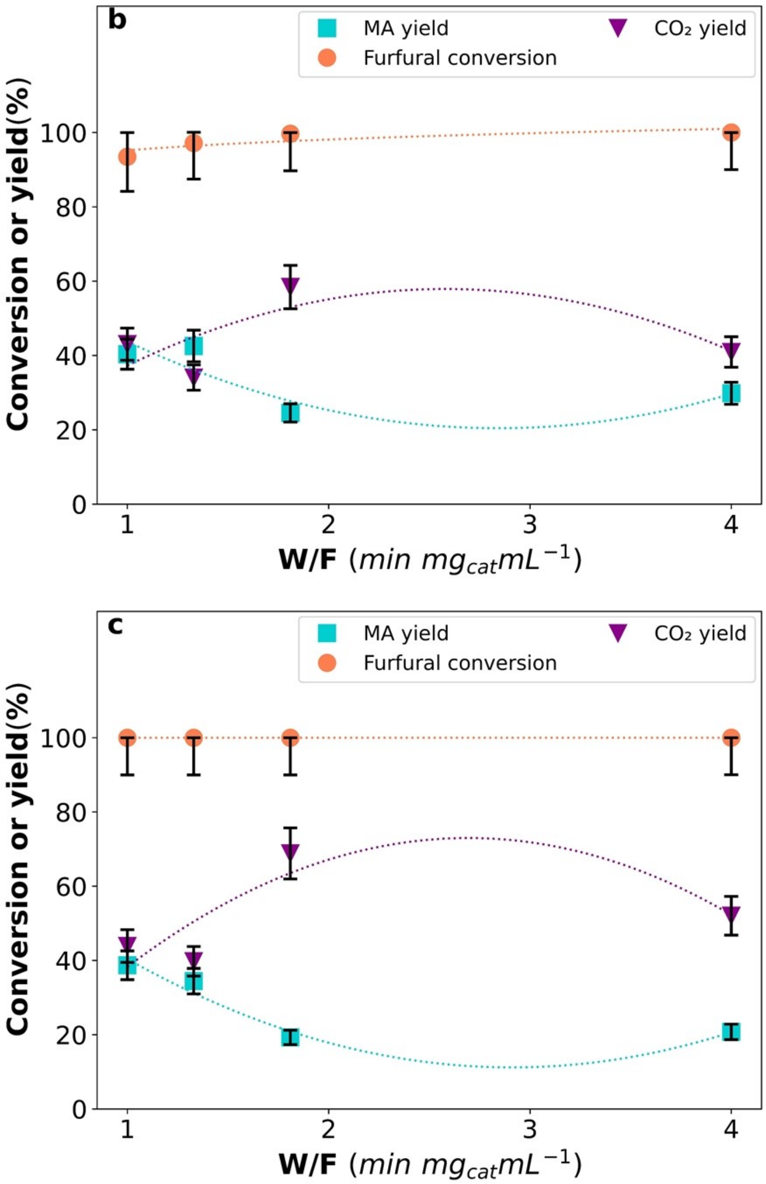

Figure S8. Effect of the of W/F ratio (1, 1.33, 1.81 and 4 min mg_{cat} mL^{-1}) at different reaction temperature (a) 280°C, (b) 300°C and (c) 320°C on furfural conversion, MA yield and CO_2 yield over V_2O_5/Al_2O_3 catalyst (P_{O2}/P_{fur}=20). The lines are added to show the trend.

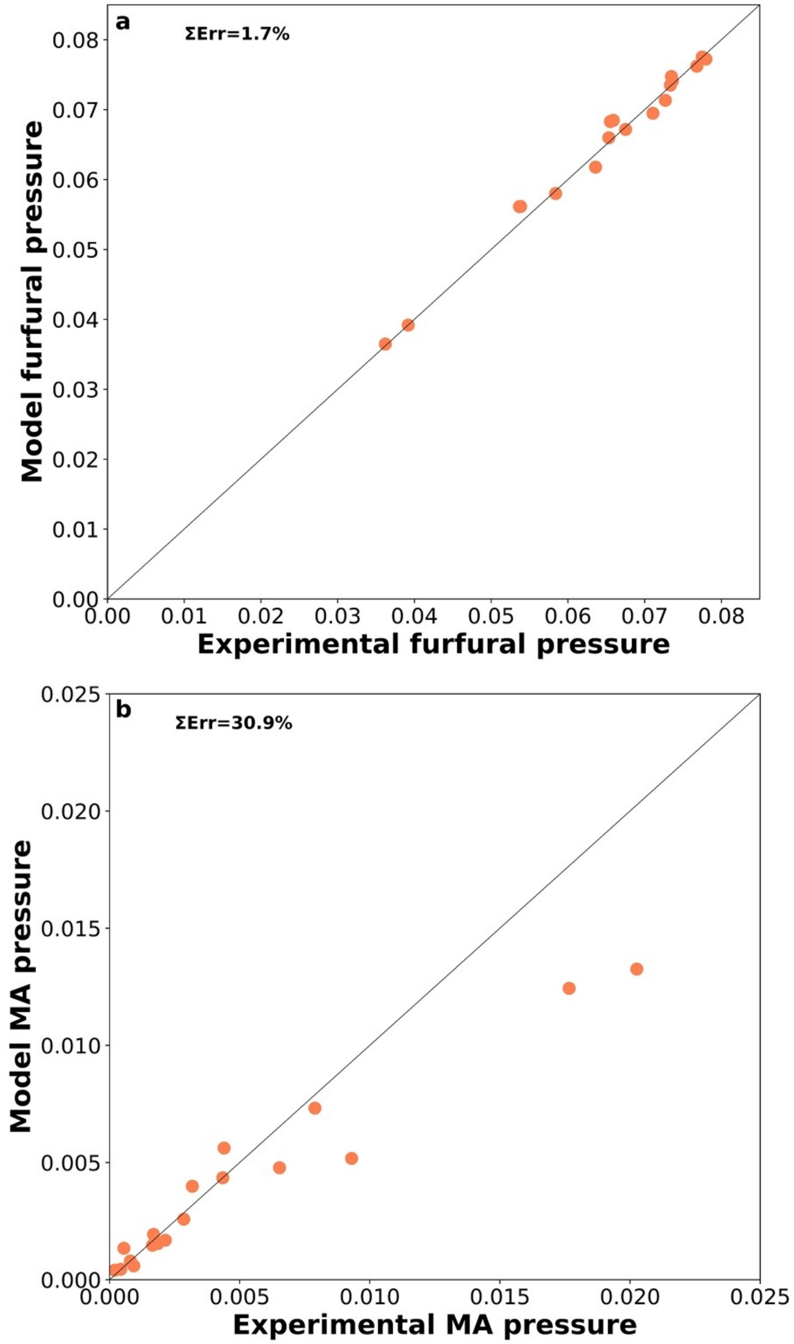

Figure S9. Parity plot for (a) furfural and (b) MA partial pressures over $VPOr_{1.0}$ catalyst obtained from the model expressed in *Eq. 4a* and *Eq. 4b*. Model consider first-order kinetics of both furfural and O_2 pressure respect to MA formation.

References

[1] H.S. Fogler, Elements of Chemical Reaction Engineering, Fourth Edi, 2006.